NASA/TM—2009-215600

Phase Fluctuations at Goldstone Derived From 1-Year Site Testing Interferometer Data

James A. Nessel and Roberto J. Acosta
Glenn Research Center, Cleveland, Ohio

David D. Morabito
Jet Propulsion Laboratory, Pasadena, California

April 2009

NASA STI Program . . . in Profile

Since its founding, NASA has been dedicated to the advancement of aeronautics and space science. The NASA Scientific and Technical Information (STI) program plays a key part in helping NASA maintain this important role.

The NASA STI Program operates under the auspices of the Agency Chief Information Officer. It collects, organizes, provides for archiving, and disseminates NASA's STI. The NASA STI program provides access to the NASA Aeronautics and Space Database and its public interface, the NASA Technical Reports Server, thus providing one of the largest collections of aeronautical and space science STI in the world. Results are published in both non-NASA channels and by NASA in the NASA STI Report Series, which includes the following report types:

- TECHNICAL PUBLICATION. Reports of completed research or a major significant phase of research that present the results of NASA programs and include extensive data or theoretical analysis. Includes compilations of significant scientific and technical data and information deemed to be of continuing reference value. NASA counterpart of peer-reviewed formal professional papers but has less stringent limitations on manuscript length and extent of graphic presentations.

- TECHNICAL MEMORANDUM. Scientific and technical findings that are preliminary or of specialized interest, e.g., quick release reports, working papers, and bibliographies that contain minimal annotation. Does not contain extensive analysis.

- CONTRACTOR REPORT. Scientific and technical findings by NASA-sponsored contractors and grantees.

- CONFERENCE PUBLICATION. Collected papers from scientific and technical conferences, symposia, seminars, or other meetings sponsored or cosponsored by NASA.

- SPECIAL PUBLICATION. Scientific, technical, or historical information from NASA programs, projects, and missions, often concerned with subjects having substantial public interest.

- TECHNICAL TRANSLATION. English-language translations of foreign scientific and technical material pertinent to NASA's mission.

Specialized services also include creating custom thesauri, building customized databases, organizing and publishing research results.

For more information about the NASA STI program, see the following:

- Access the NASA STI program home page at *http://www.sti.nasa.gov*

- E-mail your question via the Internet to *help@sti.nasa.gov*

- Fax your question to the NASA STI Help Desk at 301–621–0134

- Telephone the NASA STI Help Desk at 301–621–0390

- Write to:
  NASA Center for AeroSpace Information (CASI)
  7115 Standard Drive
  Hanover, MD 21076–1320

NASA/TM—2009-215600

Phase Fluctuations at Goldstone Derived From 1-Year Site Testing Interferometer Data

James A. Nessel and Roberto J. Acosta
Glenn Research Center, Cleveland, Ohio

David D. Morabito
Jet Propulsion Laboratory, Pasadena, California

National Aeronautics and
Space Administration

Glenn Research Center
Cleveland, Ohio 44135

April 2009

Level of Review: This material has been technically reviewed by technical management.

Available from

NASA Center for Aerospace Information
7115 Standard Drive
Hanover, MD 21076–1320

National Technical Information Service
5285 Port Royal Road
Springfield, VA 22161

Available electronically at http://gltrs.grc.nasa.gov

Phase Fluctuations at Goldstone Derived From 1-Year Site Testing Interferometer Data

James A. Nessel and Roberto J. Acosta
National Aeronautics and Space Administration
Glenn Research Center
Cleveland, Ohio 44135

David D. Morabito
National Aeronautics and Space Administration
Jet Propulsion Laboratory
Pasadena, California 91109

Abstract

A two-element site test interferometer has been deployed at the NASA Deep Space Network (DSN) tracking complex in Goldstone, California, since May 2007. The interferometer system consists of two offset-fed 1.2 m parabolic reflectors which monitor atmospheric-induced amplitude and phase fluctuations on an unmodulated beacon signal (20.199 GHz) broadcast from a geostationary satellite (Anik F2). The geometry of the satellite and the ground-based infrastructure imposes a 48.5° elevation angle with a separation distance of 256 m along an east-west baseline. The interferometer has been recording phase fluctuation data, to date, for 1 yr with an overall system availability of 95 percent. In this paper, we provide the cumulative distribution functions (CDFs) for 1 yr of recorded data, including phase *rms*, spatial structure function exponent, and surface meteorological measurements: surface wind speed, relative humidity, temperature, barometric pressure, and rain rate. Correlation between surface measurements, phase *rms*, and amplitude *rms* at different time scales are discussed. For 1 yr, phase fluctuations at the DSN site in Goldstone, are better than 23° for 90 percent of the time (at 48.5° elevation). This data will be used to determine the suitability of the Goldstone site as a location for the Next Generation Deep Space Network.

I. Introduction

As NASA progresses into the 21st century, the architecture for deep space communications is expected to undergo a radical facelift. If all proceeds as planned, the aging monolithic 34 and 70-m antennas of the Deep Space Network (DSN) are expected to be replaced with a ground-based array of up to several hundreds of smaller aperture (~12 m) antennas. The new system will provide the flexibility and reliability necessary for the demands of NASA's upcoming mission roster, reduce single-point failures, and allow electronic steering and multi-beam operational capabilities. However, the atmospheric phase stability of a particular site must be known before implementation of a ground-based array can proceed to determine the realizability of such a system.

Phase problems arise because earth's upper atmosphere (troposphere) contains large amounts of inhomogeneous distributions of water vapor exposed to turbulent air flow conditions. This property induces variations in the precipitable water vapor content, which directly leads to variations in the effective electrical path length (phase) of an electromagnetic wave propagating through this layer of the atmosphere. Such variations are seen as 'phase noise' by radio arrays and will inherently degrade the performance of widely distributed ground-based antenna systems. Further, since the troposphere is non-dispersive in phase, the phase contribution by a given amount of water vapor will increase linearly with frequency, making communications at higher frequencies (i.e., Ka-band), problematic. Radio interferometry provides the means in which these measurements can be made (ref. 1).

NASA Glenn Research Center, in collaboration with the Jet Propulsion Laboratory, has deployed a two-element site test interferometer at the Goldstone Deep Space Network Tracking Complex to accurately determine the statistical effects of precipitable water vapor on the phase stability of transmitted signals for varying baselines. One year of amplitude and phase fluctuation measurements, along with surface meteorological data, have been recorded and are presented, in a statistical fashion, in this paper. Correlation between surface measurements, phase *rms*, and amplitude *rms* at different time scales are discussed. Also, the spatial structure function exponent (α), a derived product from our analysis which determines how phase errors scale to longer (and shorter) baselines, is provided for 1 yr of data collection. The results of this analysis will directly determine the necessary system design parameters to deploy the Next Generation Deep Space Network in Goldstone.

II. Goldstone Site Test Interferometer

The GRC site test interferometer is configured at Goldstone on a 256 m east-west baseline and tracks a 20.199 GHz beacon on the geostationary communication satellite, Anik-F2, at an elevation angle of 48.5°. A full description of the interferometer hardware is provided in (ref. 2) and depicted below in Figure 1.

Each element of the interferometer consists of a 1.2 m offset-fed parabolic reflector with antenna half-power beamwidth of 0.7°. A 10 MHz GPS-disciplined Rubidium oscillator provides the reference timing for all operations. Thermal control of the Radio Frequency (RF) enclosure box and Intermediate Frequency (IF) enclosure box is maintained at an internal temperature of 49 °C, independent of outside weather conditions. The unmodulated beacon signals at 20.199 GHz are received, amplified, and down-converted in two stages: first to 70 MHz in the RF feed box, then to 455 kHz in the IF box. These 455 kHz signals are sent to the indoor facilities for Analog-to-Digital (A/D) conversion (3.64 MHz sampling rate, with 524,288 samples) and further signal processing. From the spectrum, a DSP algorithm locates the carrier peak and determines its frequency domain in-phase (I) and quadrature (Q) components. These values are stored at a sample rate of 1 Hz every 24 hr and written to a text file. Laboratory tests indicate the interferometer system is capable of resolving phase differences down to 1.8° *rms*.

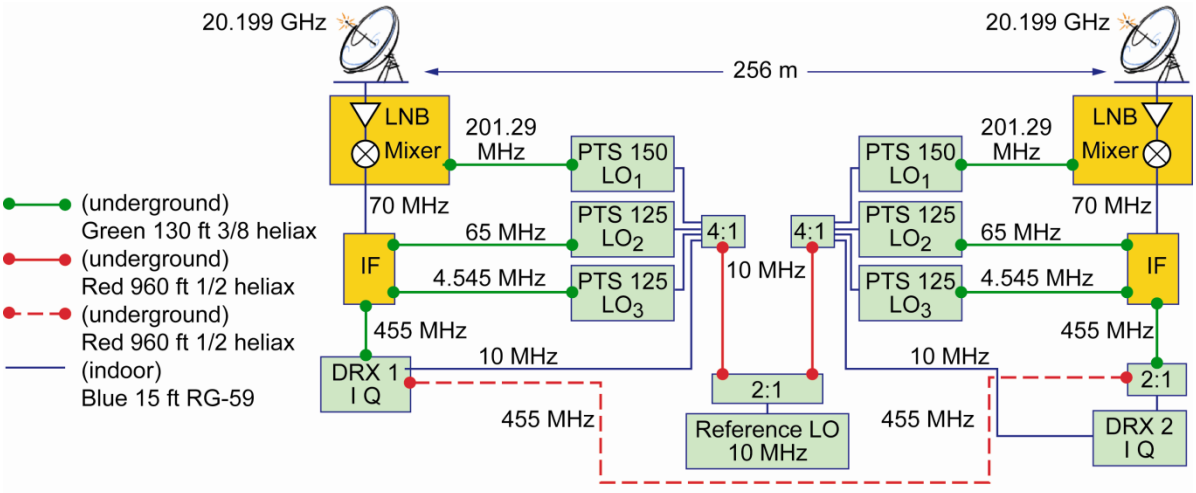

Figure 1.—Block diagram of goldstone site test interferometer.

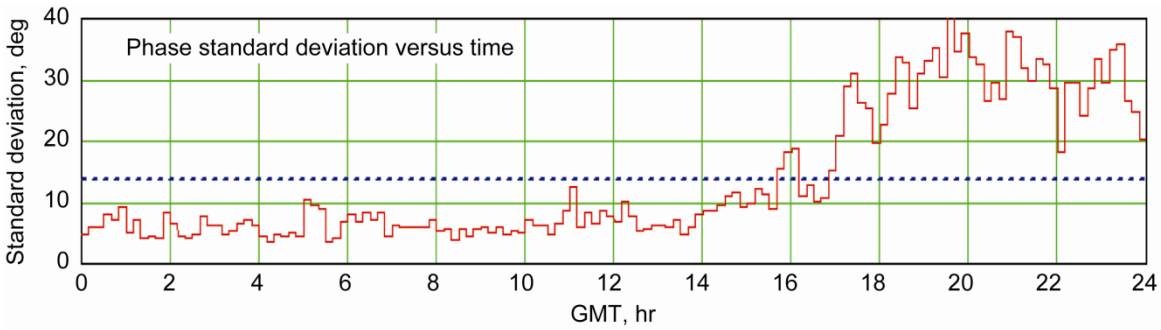

Figure 2.—Ten minute block phase standard deviation for March 1, 2008. The average phase standard deviation for the day is shown as a dashed line.

III. Data Processing

Before the data can be statistically analyzed, the phase fluctuations induced by the atmosphere must be isolated from those introduced by the system (i.e., motion of the satellite, slow varying system drift, and random system (thermal) noise). The foundation for (and validation of) this procedure can be found in (refs. 3 and 4). A summary of the steps is provided below.

First, the recorded data is unwrapped (the STI records relative phase within a ±180° range), so that a continuous differential phase curve is established. The 24-hr data is then divided into 144 blocks of 600 sec (10 min) intervals. The time scale is determined by the median wind speeds aloft (~10 m/s for Goldstone) (ref. 3). Blocks containing bad data (e.g., data recorded during maintenance visits, system-induced phase jumps, etc.) are removed. Within each good 10 min block, a 2nd order polynomial is fit to the data using a least mean square approach and subtracted, block by block. The final result of this process is the phase fluctuations due solely to the atmosphere over 10 min intervals in a given 24-hr period. From the calibrated data, the 10-min phase standard deviation is calculated as shown in Equation (1). A plot of this data is provided for March 1, 2008 in Figure 2.

$$\sigma_{\text{block}\,m} = \sqrt{\frac{\sum_{n=0+m\cdot N}^{(N-1)+m\cdot N}\left(\phi_n - \bar{\phi}_m\right)^2}{N}} \qquad \begin{array}{l} N = 600 \text{ sec} \\ m = 0\ldots143 \text{ blocks} \end{array} \tag{1}$$

In addition, the phase structure function is calculated from the recorded data to determine several other important products that aid in the understanding of the atmosphere's effects on the phase of a propagating signal for an array (refs. 5 and 6).

The spatial phase structure function is described as:

$$D_\phi(\rho) \equiv \left\langle (\phi(\rho_0) - \phi(\rho_0 + \rho))^2 \right\rangle \cong \sigma^2(\rho_0)\left(\frac{\rho}{\rho_0}\right)^{2\alpha} \tag{2}$$

where $\phi(\rho_0)$ is the phase at point ρ_0, ρ is an arbitrary baseline distance, and $\sigma^2(\rho_0)$ is the square of the *rms* phase (ref. 7). The spatial structure function tells us the distribution of phase variance as a function of the spatial scale and can be related to a temporal structure function by making use of the Taylor hypothesis or frozen phase screen model (ref. 8). Under this assumption, one can relate temporal and spatial fluctuations with a simple Eulerian transformation between baseline length and wind velocity aloft through the relationship

$$\overline{D}_\phi(t) = \sqrt{2} D_\phi(\rho)\Big|_{\rho = vt} \tag{3}$$

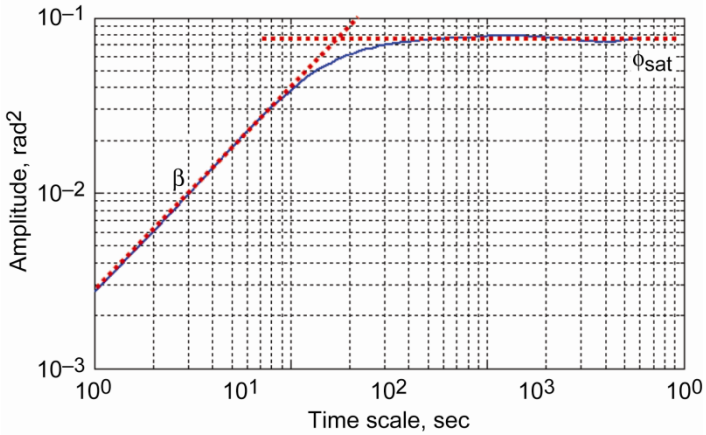

Figure 3.—Temporal phase structure function for the month of December 2007.

where v is the velocity of the phase screen aloft. From this equation, the temporal structure function is simply:

$$D_{\phi}(\tau) \equiv \left\langle (\phi(t) - \phi(t+\tau))^2 \right\rangle \cong \left(\frac{\tau}{\tau_0} \right)^{\beta} \tag{4}$$

where τ is a delay and $\phi(t)$ is the phase at time t (ref. 7). Over short time scales, the temporal phase structure function can be described by the approximation given in Equation (4) in which a power law relationship exists before saturation occurs (see plot for December 2007 in Fig. 3). The exponent of the short time scale variations is related to the spatial structure function exponent by $\beta = 2\alpha$. From this relationship, we can determine how phase *rms* scales with antenna separation distance. Over long time scales, the saturation phase *rms* (ϕ_{sat}) is a measure of the natural seeing limit of the particular site and is approximately equal to $\sqrt{2}\phi_{rms}$.

IV. 1-Year Statistics

The Cumulative Distribution Functions (CDFs) for phase standard deviation, attenuation, wind speed, temperature, relative humidity, and barometric pressure are shown in Figure 4(a) to (f), respectively, for 1 yr of data collection. The 90 percent values for each month and for the entire year are summarized in Table I. Statistically, we observe that summer months (June to September) tend to promote higher phase fluctuations than winter months (November to February). Further investigation of this phenomenon is provided in the plots of Figure 5, which shows the average hourly phase standard deviation for (a) the worst phase month (September 2007) and (b) the best phase month (November 2007). Upon closer examination, we observe that summer afternoons (17:00 to 01:00 GMT/09:00 to 17:00 PST) present the worst case phase stability throughout the year while winter nights (06:00 to 14:00 GMT/22:00 to 06:00 PST) provide the best phase stability. This general result is consistent with other interferometry measurements taken at the Very Large Array (VLA) (refs. 5 and 9) and indicates similar atmospheric patterns.

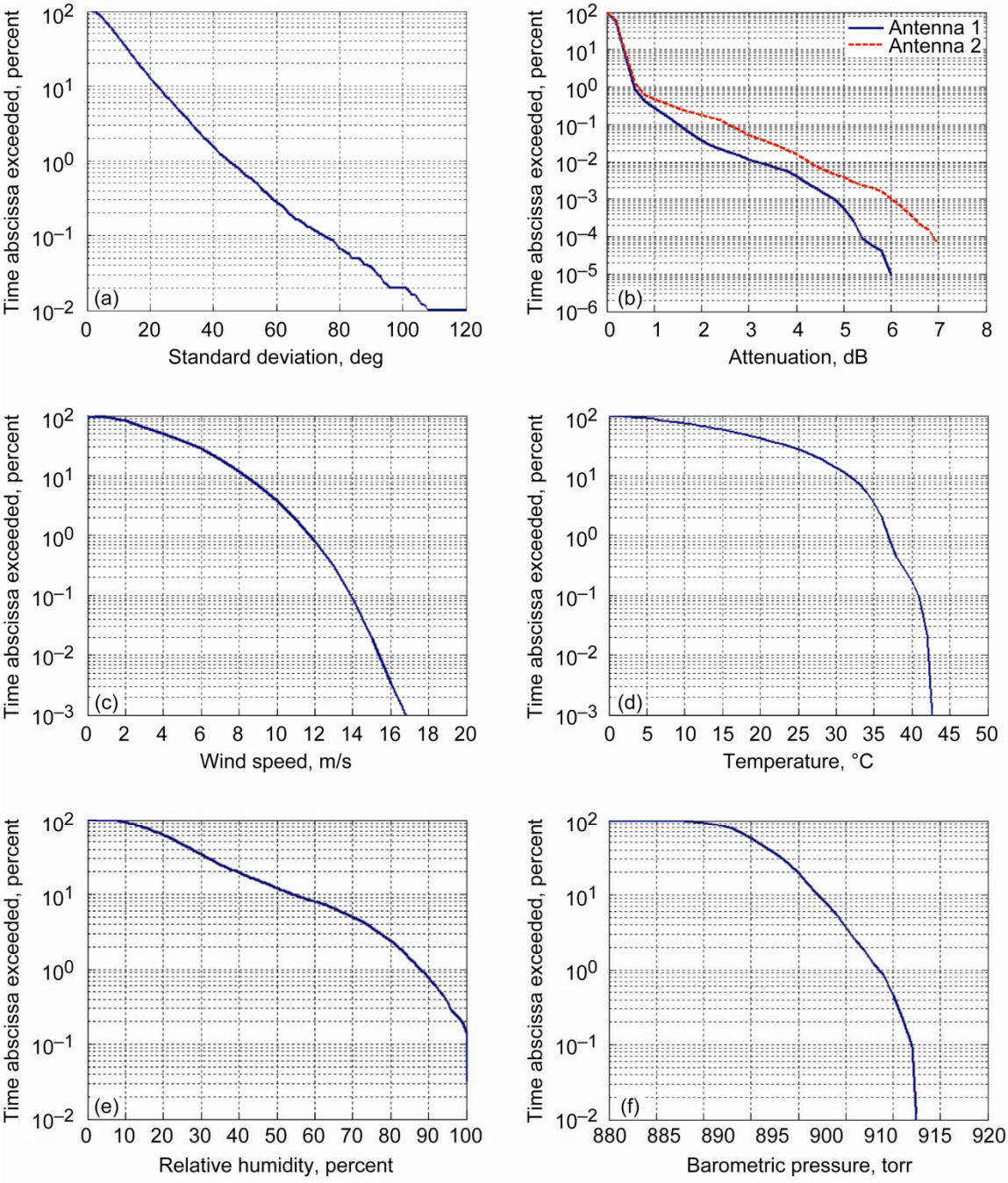

Figure 4.—One year Cumulative Distribution Functions (CDF). (a) Phase standard deviation. (b) Amplitude attenuation for each antenna. (c) Wind speed. (d) Temperature. (e) Relative humidity. (f) Barometric pressure.

Figure 6(a) shows the probability distribution of the spatial phase structure function exponent (α) for the entire year, which, as mentioned previously, relates the phase stability at a given baseline to other baselines. The median value for the year is approximately 0.53, which lies between the Kolmogorov values of 0.83 (thick atmosphere) and 0.33 (thin atmosphere) (ref. 10). This intermediate value is indicative of a superposition of the presence of a thick and thin layer at the Goldstone site. Further, the sharper cutoff in the PDF of the structure function exponent towards 0.8 reveals that the thin atmospheric layer is likely the dominant layer throughout the year. Figure 6(b) shows the cumulative distribution of the saturation phase *rms* for 1 yr. Further investigation of these parameters will be performed in later work.

TABLE 1.—NINETY PERCENT STATISTICS FOR MEASURED DATA

Month	Attenuation (dB)	Phase RMS (deg)	Wind Speed (m/s)	Temperature (°C)	Humidity (%)	Pressure (mbarr)
May 2007	----	21.33	7.9	29.5	34.5	897.0
June 2007	----	25.91	9.1	34.0	29.7	896.8
July 2007	0.54	28.50	7.7	36.5	33.7	897.0
August 2007	0.50	29.83	7.9	35.3	34.6	897.1
September 2007	0.43	29.85	7.9	32.6	57.4	898.5
October 207	0.38	21.49	9.1	23.9	50.3	904.9
November 2007	0.36	12.47	5.8	21.6	40.2	901.5
December 2007	0.37	15.95	7.5	11.4	75.4	907.0
January 2008	0.38	17.94	8.0	10.2	82.7	905.1
February 2008	0.37	17.54	8.2	16.5	72.5	903.0
March 2008	0.35	19.02	8.9	19.7	44.7	903.7
April 2008	0.34	18.88	10.2	23.3	42.1	901.5
1-yr AVG	**0.4**	**22.8**	**8.2**	**31.5**	**54**	**902.1**

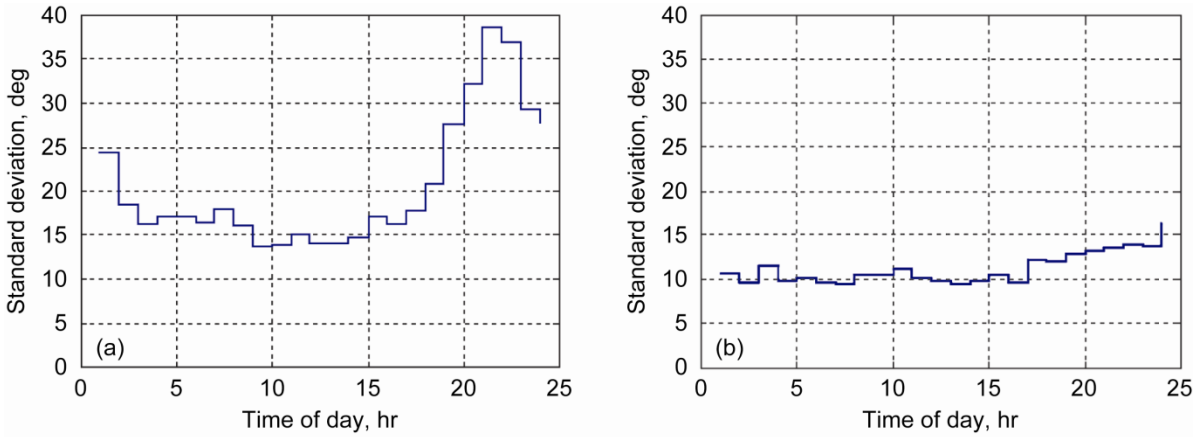

Figure 5.—Average hourly phase standard deviation time series. (a) The worst phase month, September 2007. (b) The best phase month, November 2007.

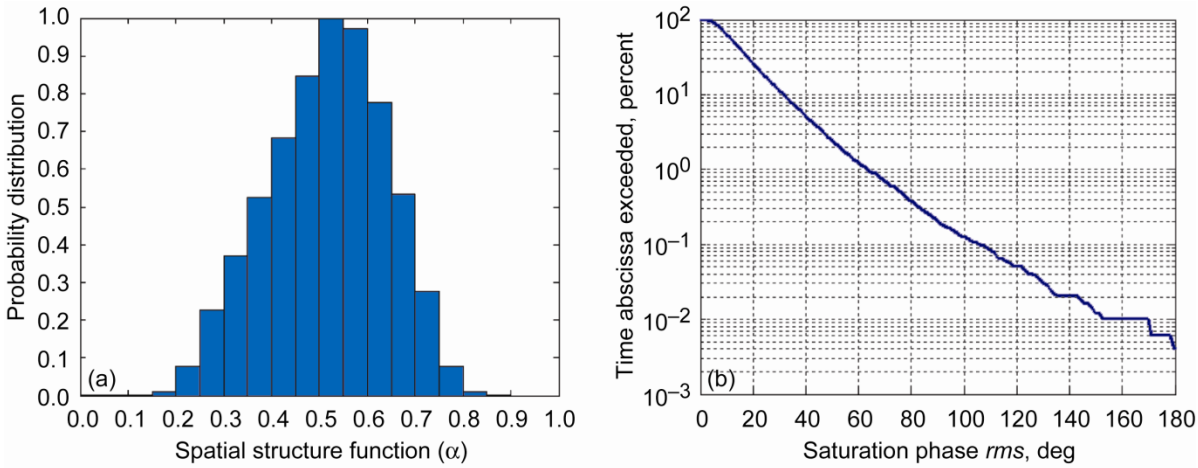

Figure 6.—(a) Probability Density Function (PDF) of the spatial phase structure function exponent (α), and (b) Cumulative Distribution Function (CDF) of saturation *rms* phase (ϕ_{sat}) for one year of data.

Based on the first year statistical results, it does not appear that there is a strong relationship (to first order) between phase fluctuations and any surface meteorological measurements taken. Further insight into a more complex relationship may be garnered through closer inspection (e.g., daily trends) of the phase and weather time series. A sample day is discussed in the next section. Application of these 1-yr statistics to determine array performance is discussed in (ref. 11).

V. Time Series Analysis (November 12, 2007)

A sample time series for November 12, 2007, is provided in this section. Phase fluctuations, attenuation, wind speed, and amplitude and phase standard deviation data are shown plotted in Figure 7. On this particular day, a cloud (possibly a rain cell) passed through the site. Also present are scintillations, appearing both throughout the day and within the cloud event. In the phase and amplitude standard deviation plots (Fig. 7, bottom graph), we observe that both amplitude and phase fluctuations increase during these scintillation events. Scintillation is, in fact, just a different manifestation of the same phenomenon that causes phase fluctuations: rapid variations in the index of refraction produced by turbulence of water vapor in the atmosphere. Other days throughout the year in which significant scintillation occurs, both amplitude and phase fluctuations show this typical response. This provides confidence that the data recorded by the interferometer are truly measurements of atmospheric-induced effects.

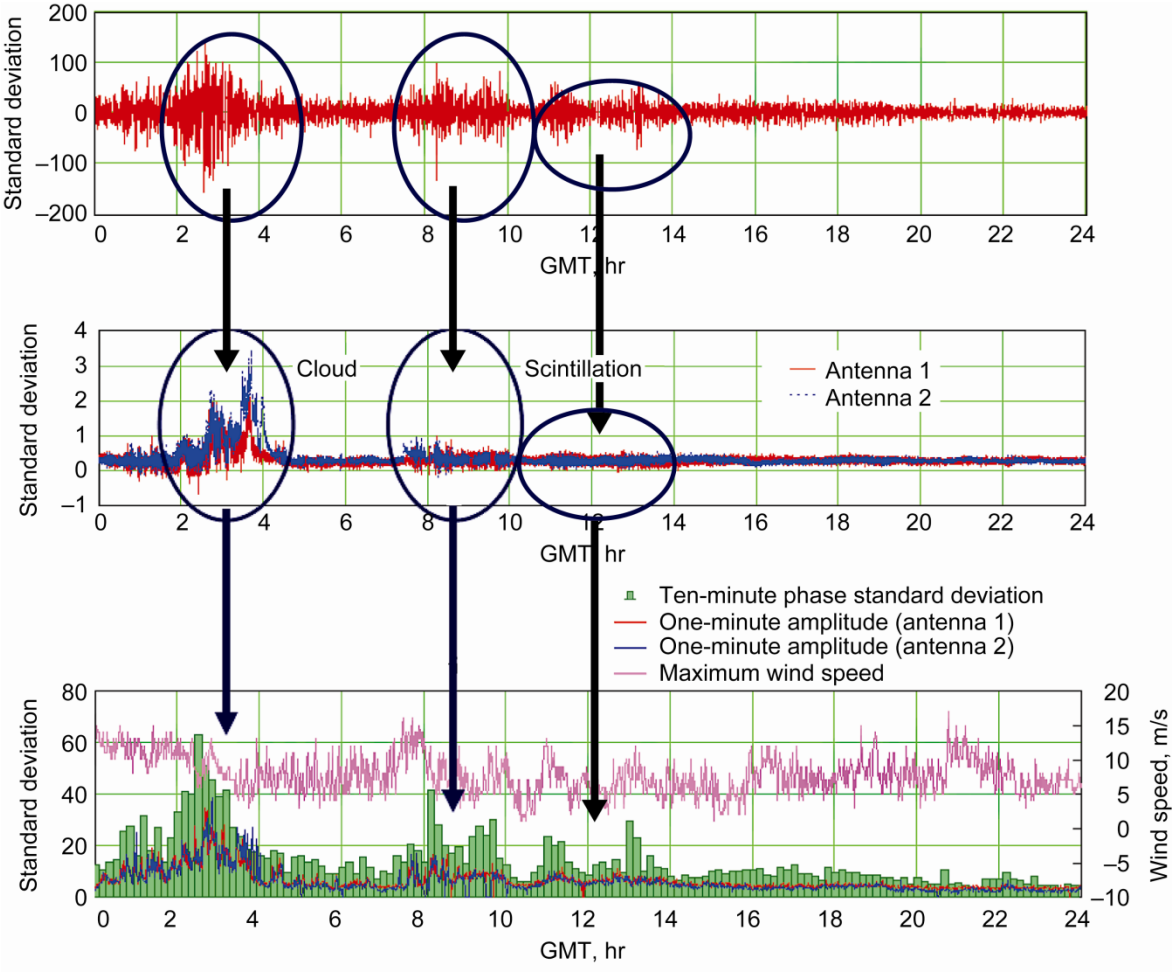

Figure 7.—Atmospheric-induced phase fluctuations (top graph), attenuation (middle graph) and amplitude and phase standard deviation curves (bottom graph) for 11/12/07. Also shown in the lower plots is the maximum surface wind speed time series.

VI. Conclusive Remarks and Future Work

From the results of the first year of data collection at Goldstone, the following conclusions can be made regarding the phase stability of the site and its potential to support a widely distributed ground-based array:

- Phase fluctuations tend to be worst during the summer months, best during winter months, and generally worse during the day than during the evening. This phenomenon is likely due to the decreased level of atmospheric turbulence in the nighttime, and especially in the wintertime.
- There does not appear to be any apparent relationship between surface meteorological data and phase fluctuations. This implies surface measurements are not accurate indicators of what is occurring higher in the atmosphere and developing a model to predict phase stability at a particular site would be extremely difficult.

Another year of phase data is presently being recorded at Goldstone, and, at the conclusion of June 2009, 2 yr of site testing interferometer data will have been collected. In addition, a radiometer has been installed at both antennas, providing another means of characterizing the atmosphere and allowing for a better understanding of atmospheric phase fluctuation phenomena. In the interim, further in-depth analysis will be performed on collected data to accurately predict array system performance and potentially develop new methods to measure atmospheric-induced phase fluctuations. Also, a second set of interferometers will be installed at the White Sands Complex, providing a comparison between two potential sites for the Next Generation Deep Space Network.

References

1. Thompson, A.R., Moran, J.M. and Swenson. G.W., "Interferometry and Synthesis in Radio Astronomy," 2nd edition, John Wiley & Sons, 2001.
2. Acosta, R.J., Frantz, B., Nessel, J.A., and Morabito, D.D., "Goldstone Site Test Interferometer," 13th Ka and Broadband Communications Conference, Turin, Italy, Sep. 24–26, 2007.
3. Nessel, J.A., Acosta, R.J., and Morabito, D.D., "Goldstone Site Test Interferometer Phase Stability Analysis," 13th Ka and Broadband Communications Conference, Turin, Italy, Sep. 24–26, 2007.
4. Acosta, R.J., Nessel, J.A., and Morabito, D.D., "Data Processing for Atmospheric Phase Interferometers," 14th Ka and Broadband Communications Conference, Matera, Italy, Sep. 24–26, 2008.
5. Butler, B., Desai, K., "Phase Fluctuation at the VLA Derived from One Year of Site Testing Interferometer Data," VLA Test Memo. no. 222, Oct. 1, 1999.
6. Holdaway, M.A., Radford, S.J., Owen, F.N., and S.M. Foster, "Data Processing for Site Test Interferometers," MMA Memo. 129, Jun. 27, 1995.
7. Tatarski V.I., 1961, Wave Propagation of the Turbulent Medium. Dover: New York.
8. Taylor, G.I., "The Spectrum of Turbulence," Proceedings of the Royal Society of London. Series A, Mathematical and Physical Sciences, Vol. 164, No. 919 (Feb. 18, 1938), pp. 476–490.
9. Sramek, R.A. "Atmospheric Phase Stability at the VLA," VLA Test Memo. no. 175, 1989.
10. D'Addario, L., "Estimates of Atmosphere-Induced Gain Loss for the Deep Space Network Array," InterPlanetary Network Progress Report 42–160, Feb. 15, 2005.
11. Morabito, D.D., D'Addario, L., Shambayati, S., Acosta, R.J., and Nessel, J.A., "Goldstone Site Test Interferometer Atmospheric Decorrelation Statistics use in Spacecraft Link Budgets: First Year of STI Data," 14th Ka and Broadband Communications Conference, Matera, Italy, Sep. 24–26, 2008.

REPORT DOCUMENTATION PAGE	Form Approved OMB No. 0704-0188

1. REPORT DATE *(DD-MM-YYYY)*	2. REPORT TYPE	3. DATES COVERED *(From - To)*
01-04-2009	Technical Memorandum	

4. TITLE AND SUBTITLE
Phase Fluctuations at Goldstone Derived From 1-Year Site Testing Interferometer Data

5a. CONTRACT NUMBER

5b. GRANT NUMBER

5c. PROGRAM ELEMENT NUMBER

6. AUTHOR(S)
Nessel, James, A.; Acosta, Roberto, J.; Morabito, David, D.

5d. PROJECT NUMBER

5e. TASK NUMBER

5f. WORK UNIT NUMBER
WBS 439432.04.12.01

7. PERFORMING ORGANIZATION NAME(S) AND ADDRESS(ES)
National Aeronautics and Space Administration
John H. Glenn Research Center at Lewis Field
Cleveland, Ohio 44135-3191

8. PERFORMING ORGANIZATION REPORT NUMBER
E-16891

9. SPONSORING/MONITORING AGENCY NAME(S) AND ADDRESS(ES)
National Aeronautics and Space Administration
Washington, DC 20546-0001

10. SPONSORING/MONITORS ACRONYM(S)
NASA

11. SPONSORING/MONITORING REPORT NUMBER
NASA/TM-2009-215600

12. DISTRIBUTION/AVAILABILITY STATEMENT
Unclassified-Unlimited
Subject Category: 32
Available electronically at http://gltrs.grc.nasa.gov
This publication is available from the NASA Center for AeroSpace Information, 301-621-0390

13. SUPPLEMENTARY NOTES

14. ABSTRACT
A two-element site test interferometer has been deployed at the NASA Deep Space Network (DSN) tracking complex in Goldstone, California, since May 2007. The interferometer system consists of two offset-fed 1.2 m parabolic reflectors which monitor atmospheric-induced amplitude and phase fluctuations on an unmodulated beacon signal (20.199 GHz) broadcast from a geostationary satellite (Anik F2). The geometry of the satellite and the ground-based infrastructure imposes a 48.5° elevation angle with a separation distance of 256 m along an east-west baseline. The interferometer has been recording phase fluctuation data, to date, for 1 yr with an overall system availability of 95 percent. In this paper, we provide the cumulative distribution functions (CDFs) for 1 year of recorded data, including phase rms, spatial structure function exponent, and surface meteorological measurements: surface wind speed, relative humidity, temperature, barometric pressure, and rain rate. Correlation between surface measurements, phase rms, and amplitude rms at different time scales are discussed. For 1 year, phase fluctuations at the DSN site in Goldstone, are better than 23° for 90 percent of the time (at 48.5° elevation). This data will be used to determine the suitability of the Goldstone site as a location for the Next Generation Deep Space Network.

15. SUBJECT TERMS
Interferometer; Deep Space Network (DSN); Goldstone; Phase stability analysis; Array; Propagation; Atmospheric effects

16. SECURITY CLASSIFICATION OF:			17. LIMITATION OF ABSTRACT	18. NUMBER OF PAGES	19a. NAME OF RESPONSIBLE PERSON
a. REPORT	b. ABSTRACT	c. THIS PAGE			STI Help Desk (email:help@sti.nasa.gov)
U	U	U	UU	14	19b. TELEPHONE NUMBER *(include area code)* 301-621-0390